490

B900 CSL

300 RM
No patent law

Coordinated Science Laboratory

UNIVERSITY OF ILLINOIS – URBANA, ILLINOIS

DESIGN AND PERFORMANCE OF A POLARITY COINCIDENCE DETECTOR

M. Raether and D. Bitzer

REPORT R-178 AUGUST, 1963

COORDINATED SCIENCE LABORATORY
UNIVERSITY OF ILLINOIS
URBANA, ILLINOIS

Contract DA-36-039-TR US AMC 02208(E)
DA Project 3A-99-25-004

The research reported in this document was made possible by support extended to the University of Illinois, Coordinated Science Laboratory, jointly by the Department of the Army, Department of the Navy (Office of Naval Research), and the Department of the Air Force (Office of Scientific Research) under Department of Army Contract DA-36-039-TR US AMC 02208(E).

ABSTRACT

A synchronous detector based on the polarity coincidence principle has been constructed and tested. The theory of operation is discussed with special emphasis on the influence of correlation between samples and the influence of error sources. Details of the construction are presented and test results are discussed. The present instrument works in the range of 20 c/sec to 20 Kc/sec and is capable of measuring signal-to-noise ratios as low as 10^{-4}. It has been in constant laboratory use for several months and has proven to be a very reliable tool for the synchronous measurement of small ac signals.

Introduction:

Synchronous detectors have received widespread application in various branches of experimental physics for the measurement of small signals in the presence of noise. Among the various schemes the Polarity Coincidence Detector (PCD) occupies a unique place because several outstanding features make it particularly suited for the measurement of very small signal-to-noise ratios.

Despite its simplicity and reliability, it has not yet found its way into laboratories as a standard research tool. It is the purpose of this report to summarize and extend the theory of operation of a PCD, and discuss the design and performance of a working model.

Historical Background:

Polarity coincidence schemes for signal detection have been proposed by several authors. Faran and Hills (1) calculated the cross correlation function of two waveforms after discarding all amplitude information. They constructed a detector where coincidences between two waveforms were produced after hard limiting. The output of the coincidence circuit was averaged by passing it through a low pass filter.

Melton and Karr (2) proposed a PCD-scheme where the waveform under consideration is sampled at appropriate time intervals and polarity coincidences are recorded. They restrict their consideration to the use of uncorrelated samples which is an unnecessary restriction. It leads to an underestimation of the statistical error.

Wolff, Thomas, and Williams (3) have shown that the polarity coincidence detector is nonparametric with respect to the "false alarm rate."

Bitzer (4) applied the polarity coincidence scheme in the space domain to phase quantization in connection with radar antennae.

In the following, the principle of operation of a PCD will be presented in a form suitable for its use as a synchronous detector for general laboratory purposes.

Theory of Operation:

A signal of known frequency may be embedded in noise. In the PCD-scheme the waveform of signal + noise is sampled with short pulses at the signal frequency. Coincidences are recorded whenever the sampled waveform and the sampling pulse have the same polarity (+ or -). With pure noise present, on the average half the samples will result in a polarity coincidence if we sample, i.e., with positive pulses.

In the presence of a signal, slightly more or less coincidences will be recorded according to the phase relationship between signal and sampling pulses.

In order to arrive at a quantitative description let us assume a signal $u\sqrt{2} \cdot \sin(\omega t + \varphi)$ in the presence of narrow band Gaussian noise,

$$x(t) = x_s \sin \omega t + x_c \cos \omega t \qquad (1)$$

where x_s and x_c are Gaussian random variables distributed according to

$$p(x_s) = \frac{1}{\sqrt{2\pi} \cdot \sigma} \exp\left(-\frac{x_s^2}{2\sigma^2}\right)$$

$$p(x_c) = \frac{1}{\sqrt{2\pi} \cdot \sigma} \exp\left(-\frac{x_c^2}{2\sigma^2}\right) . \qquad (2)$$

The sum of noise + signal can be written

$$x(t) = (x_s + u\sqrt{2}\cdot\cos\varphi)\sin\omega t + (x_c + u\sqrt{2}\ \sin\varphi)\cdot\cos\omega t$$
$$= X_s \sin\omega t + X_c\cdot\cos\omega t \quad .$$

X_s and X_c are also distributed normally, and their joint distribution is

$$p(X_s, X_c) = \frac{1}{2\pi\sigma^2}\exp\left(-\frac{X_s^2 + X_c^2}{2\sigma^2}\right) \quad .$$

We now sample in phase with X_s and X_c, respectively. A coincidence is recorded whenever the waveform exceeds a certain threshold x_+ (for positive coincidences). The fraction of sampling pulses that results in an in-phase coincidence is given by

$$\frac{n(0)}{n_o} = \frac{1}{2\pi\sigma^2}\int_{-\infty}^{+\infty}\exp\left(-\frac{(X_c - u\sqrt{2}\sin\varphi)^2}{2\sigma^2}\right)dX_c \int_{+x_+}^{\infty}\exp\left(-\frac{(X_s - u\sqrt{2}\cos\varphi)^2}{2\sigma^2}\right)dX_s$$

$$= \frac{1}{2}\left[1 - \operatorname{erf}\left(\frac{x_+}{\sigma\sqrt{2}} - \frac{u\cos\varphi}{\sigma}\right)\right] \qquad (3)$$

In an analogous way we find for sampling 90^o out-of-phase

$$\frac{n(90)}{n_o} = \frac{1}{2}\left[1 - \operatorname{erf}\left(\frac{x_+'}{\sigma\sqrt{2}} - \frac{u\sin\varphi}{\sigma}\right)\right] \quad .$$

n_o is the total number of samples in a given time,

x_+ and x_+' are usually different because different channels are involved.

For small values of the argument (small signal-to-noise ratios and hard limiting) the error function can be expanded, $\operatorname{erf}(x) \approx \frac{2x}{\sqrt{\pi}}$, and we obtain

$$\frac{n(0)}{n_o} = \frac{1}{2}\left[1 - \frac{2}{\sqrt{\pi}}\left(\frac{x_+}{\sigma\sqrt{2}} - \frac{u}{\sigma}\cos\varphi\right)\right]$$
$$\frac{n(90)}{n_o} = \frac{1}{2}\left[1 - \frac{2}{\sqrt{\pi}}\left(\frac{x_+'}{\sigma\sqrt{2}} - \frac{u}{\sigma}\sin\varphi\right)\right]. \qquad (4)$$

Let $\frac{n_N}{n_o}$ be the relative count of the noise alone. We then obtain the signal part by subtracting $\frac{n_N}{n_o}$ from $\frac{n}{n_o}$

$$\frac{1}{\sqrt{\pi}}\frac{u}{\sigma}\cos\varphi = \frac{n(0) - n_N(0)}{n_o}$$
$$\frac{1}{\sqrt{\pi}}\frac{u}{\sigma}\sin\varphi = \frac{n(90) - n_N(90)}{n_o} \qquad (5)$$

$$\frac{u}{\sqrt{\pi}\sigma} = \frac{1}{n_o}\sqrt{[n(0)-n_N(0)]^2 + [n(90)-n_N(90)]^2}\ . \qquad (6)$$

We notice that the measurement does not yield the signal itself but the signal-to-noise ratio. This has the great advantage that fluctuations in the noise level affect the measurement only slightly. The signal can still be measured as accurately as the noise is known, independent of how small the signal-to-noise ratio may actually be.

The response of the PCD is linear for small enough signal-to-noise ratios. The signal phase does not have to be known if the data are processed in the described way.

Statistical Error of the Measurement:

If all samples were statistically independent, the mean error of n counts is $\Delta n = \sqrt{n}$.

Due to the finite bandwidth of the noise, the samples are not statistically independent and the error will be larger than $\sqrt{n}$.

The variance of the sample means is given by (5)

$$\sigma_M^2 = \frac{\sigma^2}{n} + \frac{2}{n}\sum_{k=1}^{n-1} (1 - \frac{k}{n})R(kt_0). \qquad (7)$$

σ^2 is the variance of the process being sampled. $R(\tau)$ is its correlation function, N is the total number of counts. t_0 is the time between samples. $\frac{\sigma_M}{\sigma} = \frac{|\Delta n|}{n}$ is the relative error of the measurement. We can write this

$$\left|\frac{\Delta n}{n}\right|^2 = \frac{1}{n} + \frac{2}{n}\sum_{k=1}^{n-1} (1 - \frac{k}{n})\rho(kt_0) \qquad (8)$$

with $\rho(\tau) = \frac{R(\tau)}{R(0)}$ the normalized correlation function.

The correlation function for clipped signal + noise has been derived by Davenport (6) and Galejs (7). If V is the clipping level we have

$$R(\tau) = \frac{V^2}{\pi^2} \sum_{\ell=0}^{\infty} \sum_{k=0}^{\infty} \frac{1}{k!} [\sigma_N^2 \rho_N(\tau)]^k h_{\ell k}^2 \varepsilon_\ell \cos \ell\omega_0\tau. \qquad (9)$$

σ_N^2 is the variance of the noise before clipping.

$\rho_N(\tau) = \frac{R_N(\tau)}{\sigma^2}$ is the normalized correlation function of the noise before clipping.

$$\varepsilon_\ell = \begin{cases} 1 \text{ for } \ell = 0 \\ 2 \text{ for } \ell > 0 \end{cases}$$

$$h_{\ell k} = \frac{\pi\, b^{-\frac{1}{2}k} \xi^{-\frac{1}{2}\ell}}{\ell!\, \Gamma\left(\frac{2-k-\ell}{2}\right)}\, F\left(\frac{k+\ell}{2}\right);\ \ell+1;\ -\ \xi$$

F is the confluent hypergeometric function,

$b = a + \frac{1}{2}\sigma_N{}^2$ (for hard limiting $a \to 0$),

$\xi = \dfrac{u^2}{\sigma_N{}^2}$.

For small signal-to-noise ratios $\xi \ll 1$, and we may expand the hypergeometric function

$$F \approx 1 - \frac{k+\ell}{2(\ell+1)}\, \xi\ .$$

Retaining only linear terms in ξ we obtain

<u>$\ell = 0$:</u>

$$R_0 = V^2 \sum_{k=\text{odd}} \frac{1}{k!} \left[\frac{\sigma^2 \rho_N(\tau)}{b}\right]^k \frac{(1-\ k\xi)}{\Gamma^2(1-\ \frac{k}{2})}$$

with $\Gamma(1-\frac{1}{2}k) = \sqrt{\pi}\, \dfrac{(-2)^s}{1\cdot 3\cdot 5\cdots(2s-1)}$; $k = 2s+1$

$$R_0 = 2\,\frac{V^2}{\pi}\left[\left(\rho_N + \tfrac{1}{2}\,\frac{\rho_N{}^3}{3} + \frac{1}{2}\cdot\frac{3}{4}\cdot\frac{\rho_N{}^5}{5} + \cdots\right)\right.$$

$$\left. -\ \xi\left(\rho_N + \tfrac{1}{2}\,\rho_N{}^3 + \frac{1}{2}\,\frac{3}{4}\cdot\rho_N{}^5 + \cdots\ \right)\right.$$

$$= \frac{2V^2}{\pi}\left[\arcsin \rho_N - \xi\, \frac{\rho_N}{\sqrt{1-\rho_N{}^2}}\right.$$

<u>$\ell = 1$:</u>

$$R_1 = 2V^2 \sum_{k=\text{even}} \frac{1}{k!}\, \frac{2^k \rho_N{}^k \xi}{\Gamma^2(\frac{1}{2} - \frac{k}{2})} \cos \omega_o\tau$$

$$\Gamma\left(\frac{1}{2} - \frac{k}{2}\right) = \sqrt{\pi}\, \frac{(-2)^s}{1\cdot 3\cdot 5\cdots(2s-1)}\ ;\ k = 2s$$

$$R_1 = \frac{2V^2}{\pi}\,\xi\left[1 + \tfrac{1}{2}\rho_N{}^2 + \frac{1}{2}\cdot\frac{3}{4}\cdot\rho_N{}^4 + \cdots\right]\cos\omega_o\tau$$

$$= \frac{2V^2}{\pi}\,\frac{\xi}{\sqrt{1-\rho_N{}^2}}\cos\omega_o\tau.$$

Up to linear terms in ξ we obtain finally

$$R(\tau) = \frac{2V^2}{\pi}\left[\arcsin\rho_N + \xi\,\frac{\cos\omega_o\tau - \rho_N}{\sqrt{1-\rho_N{}^2}}\right]. \tag{10}$$

For a concrete example let us consider two different spectral densities of the narrow band noise. $\Delta\omega$ is defined to be the total amplitude bandwidth of the spectral density.

1. A lorentzian

$$S(\omega) = \frac{S_o}{1 + 12\,\dfrac{(\omega-\omega_o)^2}{\Delta\omega^2}} \tag{11}$$

2. A gaussian

$$S(\omega) = S_o \exp\left[-8\cdot \ell n2\,\frac{(\omega-\omega_o)^2}{\Delta\omega^2}\right].$$

1. Lorentzian

$$S_+(\omega) = \frac{S_o}{1 + 12\,\dfrac{(\omega-\omega_o)^2}{\Delta\omega^2}} \quad \text{for } \omega > 0$$

$$S_-(\omega) = \frac{S_o}{1 + 12\,\dfrac{(\omega+\omega_o)^2}{\Delta\omega^2}} \quad \text{for } \omega < 0$$

$$R_N(\tau) = \frac{1}{2\pi}\int_{-\infty}^{+\infty} S(\omega)e^{i\omega\tau}d\omega$$

We write approximately

$$R_N(\tau) = \frac{1}{2\pi}\left\{\int_{-\infty}^{+\infty} S_+(\omega)e^{i\omega\tau}d\omega + \int_{-\infty}^{+\infty} S_-(\omega)e^{i\omega\tau}d\omega\right\} = R_+ + R_- .$$

The integrals are readily evaluated by contour integration

$$\rho_N(\tau) = e^{-\frac{\Delta\omega\tau}{2\sqrt{3}}} \cdot \cos\omega_o\tau. \tag{12}$$

We obtain

$$\rho(\tau) = \frac{2}{\pi}\arcsin\left[e^{-\frac{\Delta\omega\cdot\tau}{2\sqrt{3}}} \cdot \cos\omega_o\tau\right]$$

with $\tau = kt_o$ and $t_o = \frac{2\pi}{\omega_o}$ we have

$$\left(\frac{\Delta n}{n}\right)^2 = \frac{1}{n}\left\{1 + \frac{4}{\pi}\sum_{k=1}^{n-1} \arcsin\left[e^{-\frac{\pi k\alpha}{\sqrt{3}}} \cos 2\pi k\right]\right\}$$

with $\alpha = \frac{\Delta\omega}{\omega_o}$. If α is not too small the sum converges rapidly. We define a factor β by $\Delta n = \beta\sqrt{n}$ as the factor by which the mean error is increased over the uncorrelated error. In Figure 1, β is plotted as a function of α.

2. Gaussian

$$\begin{aligned} S_+ &= S_o \exp\left[-8\,\ell n\, 2\,\frac{(\omega-\omega_o)^2}{\Delta\omega^2}\right] \quad \text{for } \omega > 0 \\ S_- &= S_o \exp\left[-8\,\ell n\, 2\,\frac{(\omega+\omega_o)^2}{\Delta\omega^2}\right] \quad \text{for } \omega < 0 \end{aligned} \tag{13}$$

$$\rho_N(\tau) = e^{-\frac{\tau^2\Delta\omega^2}{32\,\ell n\, 2}} \cdot \cos\omega_o\tau. \tag{14}$$

We obtain for $\frac{\Delta n}{n}$ in an analogous way

$$\left(\frac{\Delta n}{n}\right)^2 = \frac{1}{n}\left\{1 + \frac{4}{\pi}\sum_{k=1}^{n-1} \arcsin\left[e^{-\frac{\pi^2 k^2 \alpha^2}{8\,\ell n\, 2}} \cos 2\pi k\right]\right\}.$$

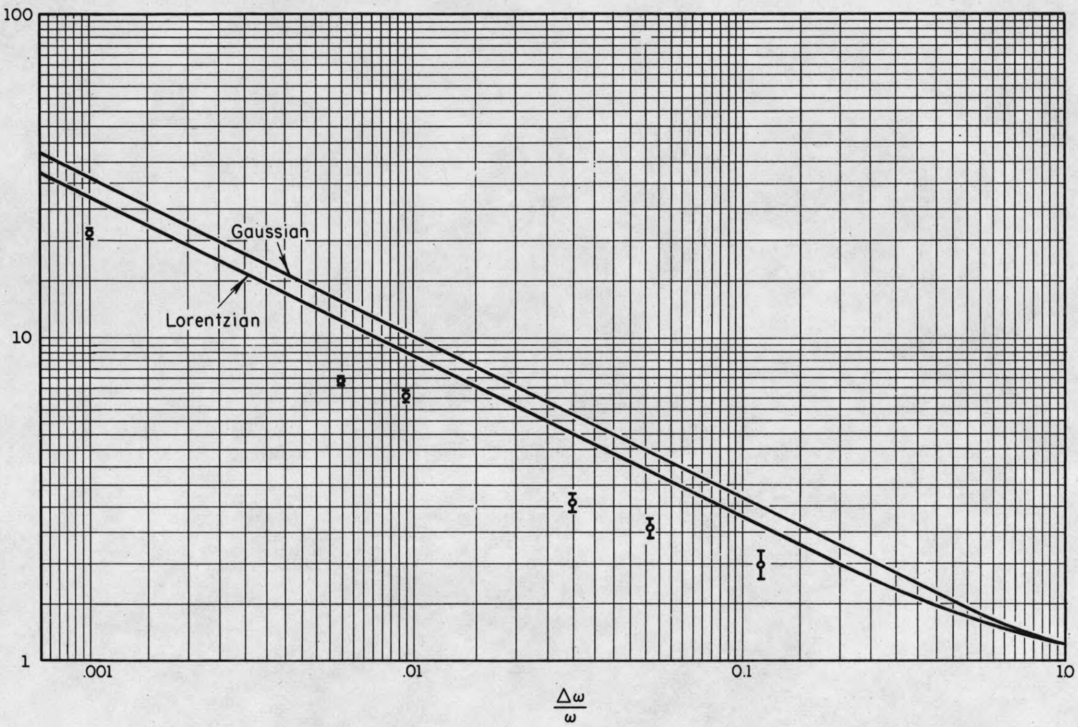

Figure 1. Statistical error as a function of bandwidth.

This sum converges very rapidly. Again, β is plotted in Figure 1.

Output Signal-to-Noise Ratio

The measurement yields the signal-to-noise ratio according to

$$\frac{u}{\sigma} = \frac{\sqrt{\pi}}{n_o} \sqrt{(n_S - n_N)_0^{\;2} + (n_S - n_N)_{90}^{\;2}} \quad . \tag{15}$$

The error of this measurement (r.m.s. deviation) for small signal-to-noise ratios is given by

$$\Delta \frac{u}{\sigma} = \sqrt{\pi} \frac{\beta}{n_o} \sqrt{n_S + n_N}$$

where β is the increase of the statistical error over the uncorrelated error $\Delta n = \beta\sqrt{n}$. $\frac{u}{\Delta u}$ can be considered as the output amplitude signal-to-noise ratio or with $S = u^2$; $N = \sigma^2$

$$\left(\frac{S}{N}\right)_{out} = \frac{(n_S - n_N)_0^{\;2} + (n_S - n_N)_{90}^{\;2}}{\beta^2 (n_S + n_N)}$$

for small signal-to-noise ratios $n_s \approx \frac{1}{2} n_o$; $n_N \approx \frac{1}{2} n_o$

$$(n_S - n_N)_0^{\;2} + (n_S - n_N)_{90}^{\;2} = \frac{n_o^{\;2}}{\pi} \left(\frac{S}{N}\right)_{in}$$

hence

$$\left(\frac{S}{N}\right)_{out} = \frac{n_o}{\pi\beta^2} \left(\frac{S}{N}\right)_{in} \quad . \tag{16}$$

We consider first the signal to be embedded in wide-band noise. The samples taken in the PCD will then be completely uncorrelated ($\beta = 1$) and the result of the measurement will be*)

$$\left(\frac{S}{N}\right)_{out} = \frac{n_o}{\pi} \left(\frac{S}{N}\right)_{in} \quad . \tag{17}$$

---

*This is only approximately true, because (15) is derived under the assumption that we are dealing with narrow-band noise.

We now pass signal + noise through a filter with a system function $H(i\omega)$ which reduces the variance of the input noise, but in consequence introduces correlation between adjacent samples.

$$\left(\frac{S}{N}\right)_{out} = \frac{n_o}{\pi\beta^2}\left(\frac{S}{N}\right)_F$$

where $\left(\frac{S}{N}\right)_F$ is the signal-to-noise ratio at the output of the filter. The filter does not act on the signal but only on the noise.

Let $G_{in}(\omega)$ be the spectral density at the input, $G_o(\omega)$ the spectral density at the output, then

$$G_o(\omega) = |H(i\omega)|^2 G_{in}(\omega)$$

$$N = \frac{1}{2\pi}\int_{-\infty}^{+\infty} G(\omega)d\omega$$

hence

$$\left(\frac{S}{N}\right)_F = \frac{S}{\frac{1}{2\pi}\int_{-\infty}^{+\infty}|H(i\omega)|^2 G_{in}(\omega)d\omega}$$

or since

$$N_{in} = \frac{1}{2\pi}\int_{-\infty}^{+\infty} G_{in}(\omega)d\omega$$

$$\left(\frac{S}{N}\right)_F = \left(\frac{S}{N}\right)_{in}\frac{\int_{-\infty}^{+\infty} G_{in}(\omega)d\omega}{\int_{-\infty}^{+\infty}|H(i\omega)|^2 G_{in}(i\omega)d\omega}$$

$$\left(\frac{S}{N}\right)_{out} = \frac{n_o}{\pi\beta^2}\frac{\int_{-\infty}^{+\infty} G_{in}(\omega)d\omega}{\int_{-\infty}^{+\infty}|H(i\omega)|^2 G_{in}(\omega)d\omega}\left(\frac{S}{N}\right)_{in}.$$

Let us consider white input noise up to a frequency ω_N

$$G(\omega) = G_o \quad \text{for} \quad \omega \le \omega_N$$

$$= 0 \quad \text{for} \quad \omega > \omega_N$$

and a system function $H(i\omega) = 1$ for $\omega_o - \frac{1}{2}\Delta\omega < \omega < \omega_o + \frac{1}{2}\Delta\omega$

$= 0$ for outside.

This results in

$$\left(\frac{S}{N}\right)_{out} = \frac{n_o}{\pi\beta^2} \frac{\omega_N}{\Delta\omega} \left(\frac{S}{N}\right)_{in} \tag{18}$$

for small values of $\frac{\Delta\omega}{\omega_o}$

$$\beta \sim \sqrt{\frac{\omega_o}{\Delta\omega}} .$$

We notice that there is an advantage to filter out frequencies $> \omega_o$ before coincidence detection. Nothing, however, is gained by filtering out low frequencies, except near zero. A band-pass filter of width $-\omega_o$ is equally as effective as a narrow band-pass filter.

The necessity for introducing a filter before coincidence detection arises because the signal is sampled at a low rate. The effect of sampling can be illustrated more easily if the coincidence detector is replaced by a linear integrator. In the linear integrator the amplitude of the signal at the instant of sampling are summed as compared to the polarity coincidence detector where the amplitudes are converted to $\pm$ 1 before summing. The effect of summing the sampled signal is the same as transmitting the original signal through a comb filter. The center frequencies of the pass bands are separated from the neighboring bands by ω_o, where ω_o is the sampling rate. The width of each pass band is approximately the reciprocal of the total integration time. Since the desired part of the signal is monochromatic at frequency ω_o, it is desirable to filter out all of the pass bands except the band centered at ω_o. This can be accomplished by using a filter of width ω_o.

Experimental Part:

The technical realization of the polarity coincidence principle presents no essential problems. Figure 2 shows the block diagram of an operational model that is presently in laboratory use for several months. The use of a synchronous detector in an experiment usually proceeds in the following way. A generalized carrier (which can be an rf-signal, an electron beam, a molecular beam, and so forth) interacts with the system under investigation. If the carrier is modulated with a certain frequency any change in the system that results from the interaction will exhibit the same frequency component. This change is detected and transformed into an ac signal which is cross-correlated with the modulation frequency.

In the case of the polarity coincidence detector, the signal is passed through a limiting amplifier. In the present model the limiting amplifier consists of three wideband feedback loops with an individual gain of 50 and a rise time of 0.1 microsecond. Limiting is accomplished by a pair of biased diodes after each stage. The output is a square wave of 40 V_{pp} amplitude.

The reference signal is split into two channels 90^{o} out of phase, where it is converted into sampling pulses of 0.5 microsecond duration. Sampling pulses and output of the limiting amplifier are applied to the two control grids of 6BN6 tube. The output of the coincidence tubes triggers multivibrators that generate standard pulses for the counters. In order to cancel out fluctuations in bias level or noise level, signal + noise is counted for a given time determined by a pre-set count of the master counter. The modulation is switched off and the noise alone is recorded for the same time on a different set of counters. The noise + signal and the noise counts alternate typically every 10 seconds.

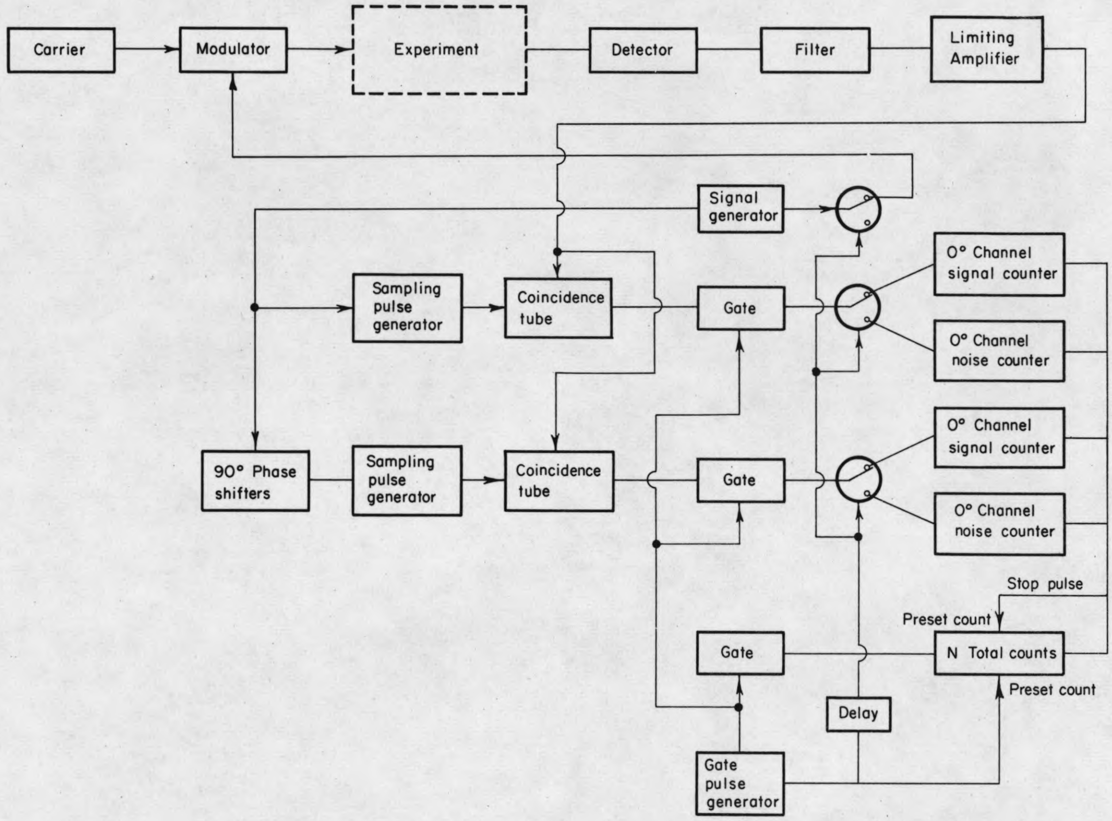

Figure 2. Schematic diagram of polarity coincidence detector.

The instrument operates in the range 20 c/sec-20 kc/sec. The performance is demonstrated by the following set of diagrams.

Figure 3 shows a plot of the output signal, defined as $\sqrt{(n_S-n_N)_0^{\,2} + (n_S-n_N)_{90}^{\,2}}$ in arbitrary units versus the input amplitude signal-to-noise ratio. The signal frequency was 10 kc/sec. We notice the deviation from linearity for signal-to-noise ratios larger than 0.2.

The response of the individual channels to a phase shift between signal and reference signal is demonstrated by Figure 4, where the counting rates of the individual channels are plotted versus the phase shift between signal and reference signal. The signal-to-noise ratio was 0.05, frequency 10 kc. The measured values fit smoothly a sin and cos dependence.

In order to check the increase of the error with decreasing bandwidth of the noise, series of 50 individual readings of the counting rate were taken. The computed statistical error of a single reading together with its error is plotted in Figure 1 versus the relative bandwidth of the noise. Although the error is smaller than predicted for a Lorentzian or Gaussian spectral density, the qualitative behavior is confirmed.

The appendix contains the complete circuit diagrams of the instrument.

Error Sources:

a) Fluctuations of threshold:

The main uncertainty is introduced in the first limiting stage of the amplifier. We have

$$\frac{n(0)}{n_o} = \frac{1}{2}\left[1 - \frac{2x_+}{\sqrt{2\pi}\cdot\sigma} + \frac{2u}{\sigma\sqrt{\pi}}\cos\varphi\right]$$

$$\frac{\Delta n(0)}{n_o} = \frac{\Delta x_+}{\sigma\sqrt{2\pi}} \,.$$

σ is the variance of the noise after amplification by the first stage.

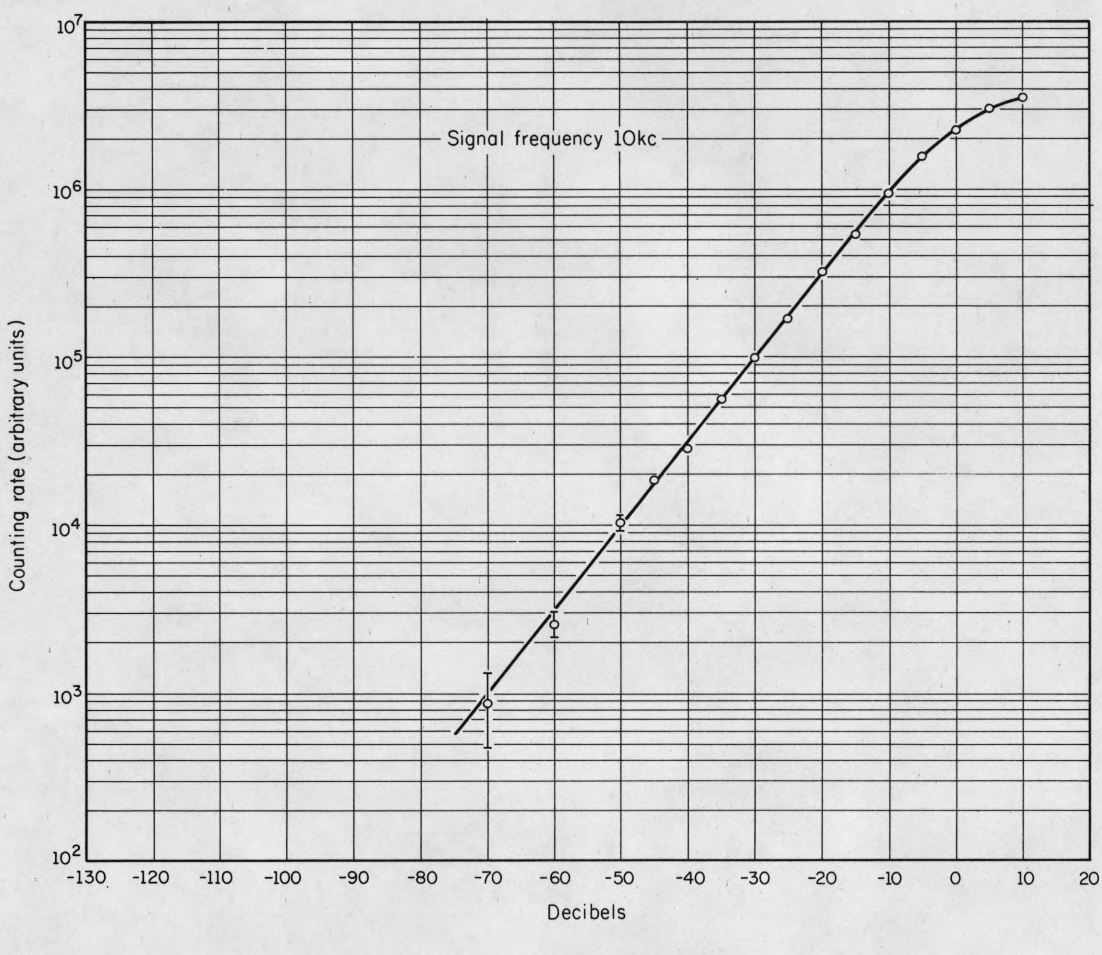

Figure 3. Response of polarity coincidence detector to input signal-to-noise ratio. (0 db corresponds to S/N=1)

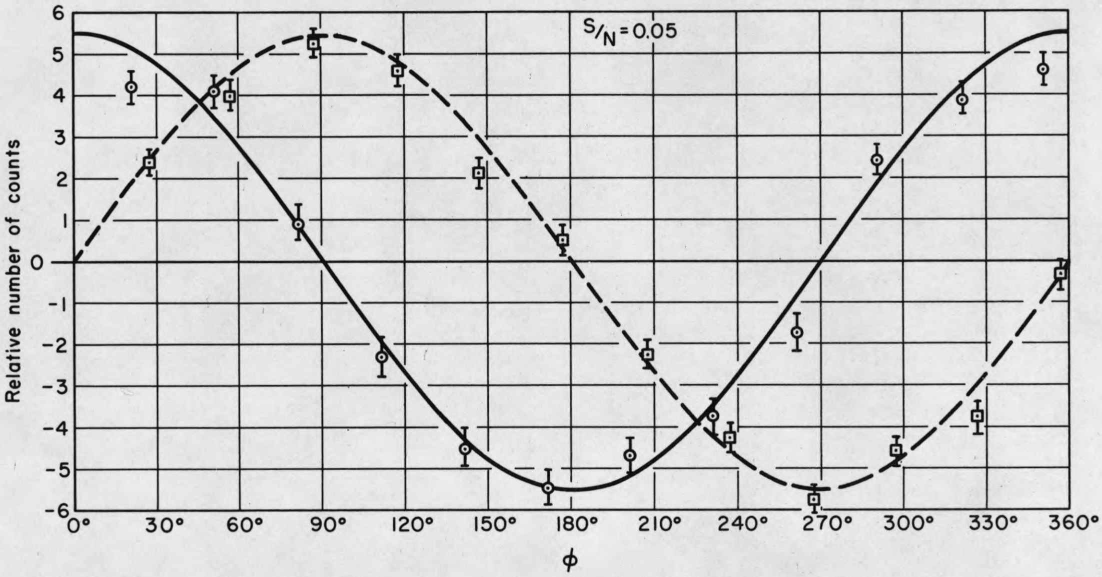

Figure 4. Counting rate as a function of phase shift between signal and reference signal.

The error of the measurement can then be written

$$\Delta \frac{u}{\sigma\sqrt{\pi}} = \sqrt{\frac{\beta^2}{n_o} + \frac{\Delta x_+^{\,2} + \Delta x_+^{\prime\,2}}{2\pi\sigma^2}} \; . \qquad (19)$$

The conditions for the influence of the threshold fluctuation to be small compared to the statistical error can then be written

$$\frac{(\Delta x)^2}{\pi\sigma^2} < \frac{\beta^2}{n_o} \; .$$

σ is limited by the dynamical range of the amplifier. In a typical example one may have $\sigma = 100V$

$\Delta x = 0.1V$

$\beta = \sqrt{2}$. This requires $n_o < 6 \times 10^6$, and the minimum detectable signal-to-noise ratio would be 5×10^{-5}.

b) Phase Fluctuations:

When the signal is passed through narrow band filters the possibility of phase fluctuations must be considered. We have

$$\Delta n(0) = -n_o \frac{u}{\sigma\sqrt{\pi}} \cos\varphi \cdot \Delta\varphi$$

$$\Delta n(90) = n_o \frac{u}{\sigma\sqrt{\pi}} \sin\varphi \cdot \Delta\varphi \; .$$

This contributes to the error according to

$$\Delta \frac{u}{\sigma\sqrt{\pi}} = \sqrt{\frac{\beta^2}{n_o} + \frac{u^2}{\pi\sigma^2}\,\Delta\varphi^2} \; . \qquad (20)$$

In the limiting case $n_o \to \infty$ we have $\frac{\Delta u}{u} = \Delta\varphi$. The influence of phase fluctuations is negligible in most situations.

c) Noise Fluctuations:

A fluctuation in the noise level changes the counting rate by

$$\frac{\Delta n_S(0)}{n_o} = \frac{1}{\sqrt{\pi}} \left(\frac{x_+}{\sqrt{2}} - u\cos\varphi\right) \frac{\Delta\sigma}{\sigma^2} .$$

An analogous expression holds for $\Delta n_s(90)$.

The error in the signal-to-noise ratio becomes

$$\Delta\left(\frac{u}{\sigma}\right) = \sqrt{\pi} \sqrt{\frac{\beta^2}{n_o} + \frac{\Delta\sigma^2}{n_o^2 u^2 \sigma^2} \left\{ (n_S - n_N)_0^2 \left[\frac{x_+^2}{2} + \left(\frac{x_+}{\sqrt{2}} - u\cos\varphi\right)^2\right] + (n_S - n_N)_{90}^2 \left[\frac{x_+'^2}{2} + \left(\frac{x_+'}{\sqrt{2}} - u\sin\varphi\right)^2\right] \right\}} .$$

In two limiting cases this simplifies considerably

1) $u \ll x_+ \qquad x_+ \approx x_+' = x$

$$\Delta\frac{u}{\sigma} = \sqrt{\pi} \sqrt{\frac{\beta^2}{n_o} + \frac{1}{\pi} \frac{x^2}{\sigma^2} \left(\frac{\Delta\sigma}{\sigma}\right)^2} . \tag{21}$$

The minimum detectable signal-to-noise ratio then becomes

$$\left(\frac{u}{\sigma}\right)_{min} = \frac{x}{\sigma} \cdot \frac{\Delta\sigma}{\sigma} .$$

2) $u \gg x_+$

$$\Delta\frac{u}{\sigma} = \sqrt{\pi} \sqrt{\frac{\beta^2}{n_o} + \frac{1}{\pi} \frac{u^2}{\sigma^2} \left(\frac{\Delta\sigma}{\sigma}\right)^2 (\cos^4\varphi + \sin^4\varphi)} . \tag{22}$$

The minimum relative error becomes

$$\frac{\Delta u}{u} = \frac{\Delta\sigma}{\sigma} \sqrt{\cos^4\varphi + \sin^4\varphi} .$$

$\sqrt{\cos^4\varphi + \sin^4\varphi}$ varies between 1 and $\frac{1}{\sqrt{2}}$.

d) Linearity:

In order to get an estimate of the deviation of the measurement from linearity we expand the error function in the expression for $\frac{n_S(0)}{n_o}$.

$$\frac{n_S(0)}{n_o} \approx \frac{1}{2}\left[1 - \frac{2}{\sqrt{\pi}}\left(\frac{x}{\sigma\sqrt{2}} - \frac{u}{\sigma}\cos\varphi\right) - \frac{2}{3\sqrt{\pi}}\left(\frac{x}{\sigma\sqrt{2}} - \frac{u}{\sigma}\cos\varphi\right)^3 + \cdots\right]$$

$$\frac{n_N(0)}{n_o} \approx \frac{1}{2}\left[1 - \frac{2}{\sqrt{\pi}}\frac{x}{\sigma\sqrt{2}} - \frac{2}{3\sqrt{\pi}}\frac{x^3}{\sigma^3 2^{3/2}} - \cdots\right]$$

$$\frac{n_S - n_N}{n_o} = \frac{u}{\sqrt{\pi}\,\sigma}\left[1 + \left(\frac{u}{\sqrt{\pi}\,\sigma}\right)^2 + \cdots\right] .$$

For a signal-to-noise ratio of 0.1, i.e., the deviation from linearity is less than one per cent.

We are indebted to Professor D. Cooper for valuable discussions on the subject of signal detection.

REFERENCES

1) J. J. Faran and R. Hills, Tech. Memo No. 27, Acoustic Research Lab., Harvard University (1952).

2) B. S. Milton and P. R. Karr, Geophysics 22, 553 (1957).

3) S. S. Wolff, J. B. Thomas, T. R. Williams, IRE Trans. T8, 5 (1962).

4) D. L. Bitzer, Ph.D. Thesis, University of Illinois (Dec., 1959).

5) W. R. Davenport, Jr. and W. L. Root. An Introduction to the Theory of Random Signals and Noise, (McGraw-Hill, 1958).

6) W. B. Davenport, J. Appl. Phys. 29, 720 (1953).

7) J. Galejs, IRE Transactions Information Theory 1T, 5, 79 (1959).

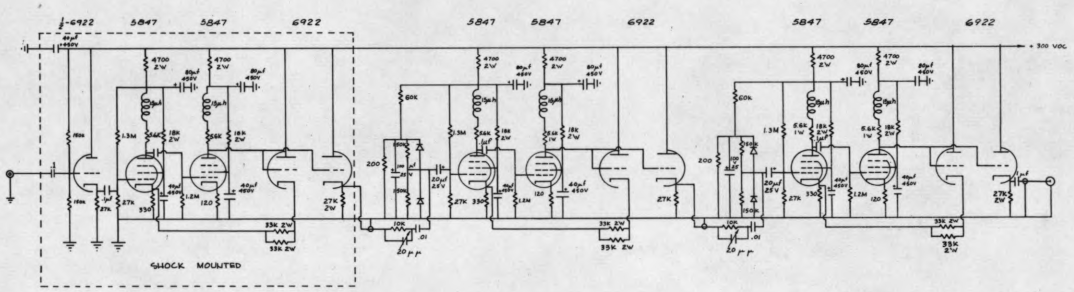

NOTES

1. ALL DIODES 1N661
2. FILAMENTS 6.3 VDC AND BYPASSED BY 33 $\mu\mu$ AT EACH SOCKET
3. FILAMENT LEAD Gnd AT FIRST AMP. TUBE
4. ALL CONTROL GRIDS HAVE A SERIES 47 Ω RESISTOR

Figure 1 (Appendix). Limiting Amplifier.

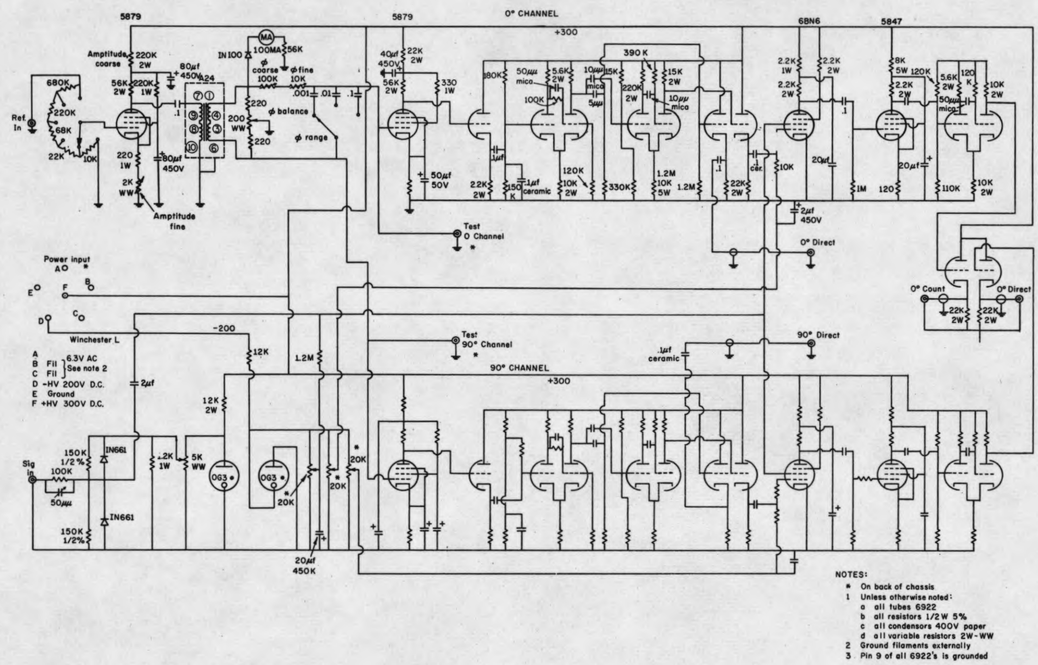

Figure 2 (Appendix). Coincidence Circuit.

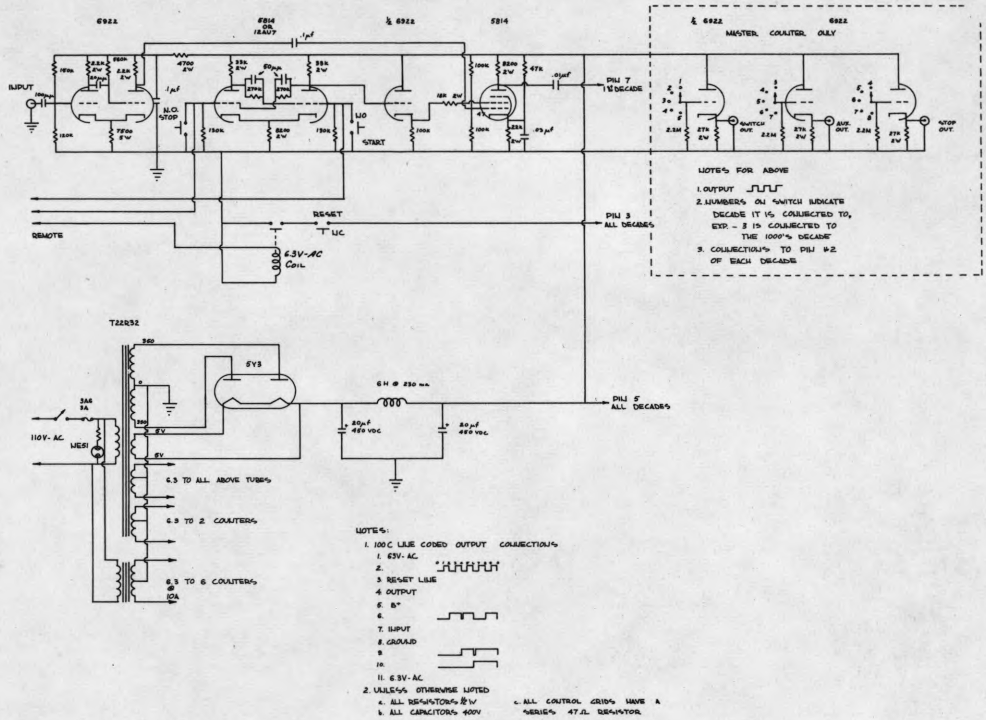

Figure 3 (Appendix). Counter.

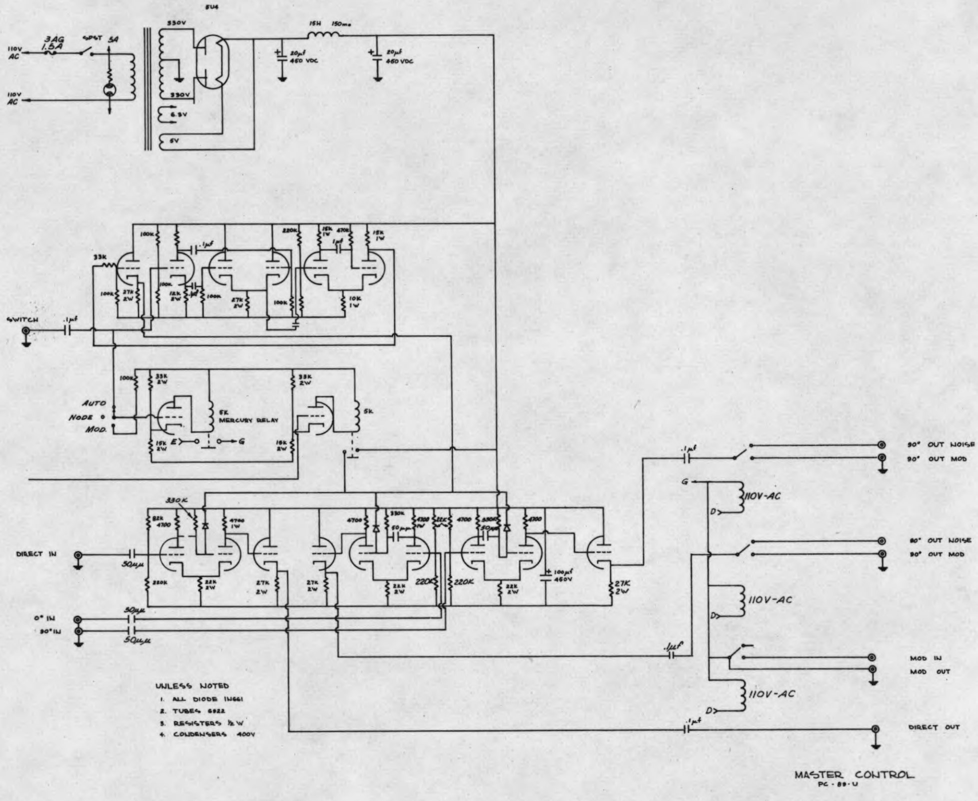

Figure 4 (Appendix). Master Control.

DISTRIBUTION LIST AS OF JULY 12, 1963

1 Director
Air University Library
Maxwell Air Force Base, Alabama
Attn: CR-4803a

1 Redstone Scientific Information Center
U.S. Army Missile Command
Redstone Arsenal, Alabama

1 Electronics Research Laboratory
University of California
Berkeley 4, California

2 Hughes Aircraft Company
Florence and Teale
Culver City, California
Attn: N. E. Devereux
Technical Document Center

3 Autonetics
9150 East Imperial Highway
Downey, California
Attn: Tech. Library, 3041-11

1 Dr. Arnold T. Nordsieck
General Motors Corporation
Defense Research Laboratories
6767 Hollister Avenue
Goleta, California

1 University of California
Lawrence Radiation Laboratory
P. O. Box 808
Livermore, California

1 Mr. Thomas L. Hartwick
Aerospace Corporation
P. O. Box 95085
Los Angeles 45, California

1 Lt. Colonel Willard Levin
Aerospace Corporation
P. O. Box 95085
Los Angeles 45, California

1 Professor Zorab Kaprelian
University of Southern California
University Park
Los Angeles 7, California

1 Sylvania Electronic Systems - West
Electronic Defense Laboratories
P. O. Box 205
Mountain View, California
Attn: Documents Center

1 Varian Associates
611 Hansen Way
Palo Alto, California
Attn: Dr. Ira Weissman

1 Huston Denslow
Library Supervisor
Jet Propulsion Laboratory
California Institute of Technology
Pasadena, California

1 Professor Nicholas George
California Institute of Technology
Electrical Engineering Department
Pasadena, California

1 Space Technology Labs., Inc.
One Space Park
Redondo Beach, California
Attn: Acquisitions Group
STL Technical Library

2 Commanding Officer and Director
U.S. Naval Electronics Laboratory
San Diego 52, California
Attn: Code 2800, C. S. Manning

1 Commanding Officer and Director
U.S. Navy Electronics Laboratory
San Diego 52, California
Attn: Library

1 Office of Naval Research Branch Office
1000 Geary Street
San Francisco, California

1 The RAND Corporation
1700 Main Street
Santa Monica, California
Attn: Library

1 Stanford Electronics Laboratories
Stanford University
Stanford, California
Attn: SEL Documents Librarian

1 Dr. L. F. Carter
Chief Scientist Air Force
Room 4E-324, Pentagon
Washington 25, D. C.

1 Mr. Robert L. Feik
Associate Director for Research
Research and Technology Division
AFSC
Bolling Air Force Base 25, D. C.

1 Captain Paul Johnson (USN-Ret)
National Aeronautics and Space
Administration
1520 H Street, N. W.
Washington 25, D. C.

1 Major Edwin M. Myers
Headquarters USAF (AFRDR)
Washington 25, D. C.

1 Dr. James Ward
Office of Deputy Director
(Research and Info)
Department of Defense
Washington 25, D. C.

1 Dr. Alan T. Waterman
Director, National Science Foundation
Washington 25, D. C.

1 Mr. G. D. Watson
Defense Research Member
Canadian Joint Staff
2450 Massachusetts Ave., N. W.
Washington 8, D. C.

1 Mr. Arthur G. Wimer
Chief Scientist
Air Force Systems Command
Andrews Air Force Base
Washington 25, D. C.

1 Director, Advanced Research
Projects Agency
Washington 25, D. C.

1 Air Force Office of Scientific Branch
Directorate of Engineering Sciences
Washington 25, D. C.
Attn: Electronics Division

1 Director of Science and Technology
Headquarters, USAF
Washington 25, D. C.
Attn: AFRST-EL/GU

1 Director of Science and Technology
AFRST - SC
Headquarters, USAF
Washington 25, D. C.

1 Headquarters, R & T Division
Bolling Air Force Base
Washington 25, D. C.
Attn: RTHR

1 Headquarters, U.S. Army Material Command
Research Division, R & D Directorate
Washington 25, D. C.
Attn: Physics & Electronics Branch
Electronics Section

1 Commanding Officer
Diamond Ordnance Fuze Laboratories
Washington 25, D. C.
Attn: Librarian, Room 211, Bldg. 92

1 Operations Evaluation Group
Office of the CNO (Op03EG)
Navy Department
Washington 25, D. C.

1 Chief of Naval Operations
Tech. Analysis & Advisory Group (OP-07T)
Pentagon
Washington 25, D. C.

1 Commanding Officer
U.S. Army Personnel Research Office
Washington 25, D. C.

1 Commanding Officer & Director
David W. Taylor Model Basin
Navy Department
Washington 7, D. C.
Attn: Code 142, Library

1 Bureau of Ships
Department of the Navy
Washington 25, D. C.
Attn: Code 686

1 Bureau of Ships
Navy Department
Washington 25, D. C.
Attn: Code 732

1 Technical Library, DLI-3
Bureau of Naval Weapons
Department of the Navy
Washington 25, D. C.

1 Director
Naval Research Laboratory
Washington 25, D. C.
Attn: Code 5140

1 Department of the Navy
Office of Naval Research
Washington 25, D. C.
Attn: Code 437

1 Dr. H. Wallace Sinaiko
Institute for Defense Analyses
Research & Engineering Support Division
1666 Connecticut Ave., N.W.
Washington 9, D. C.

1 Data Processing Systems Division
National Bureau of Standards
Conn. at Van Ness
Room 239, Bldg. 10
Washington 25, D. C.
Attn: A. K. Smilow

1 Exchange and Gift Division
The Library of Congress
Washington 25, D. C.

1 NASA Headquarters
Office of Applications
400 Maryland Avenue, S.W.
Washington 25, D. C.
Attn: Mr. A. M. Greg Andrus
Code FC

1 AOGC (PGAPI)
Eglin Air Force Base
Florida

1 Commanding Officer
Office of Naval Research, Chicago Branch
6th Floor, 230 North Michigan
Chicago 1, Illinois

1 Laboratories for Applied Sciences
University of Chicago
6220 South Drexel
Chicago 37, Illinois

1 Librarian
School of Electrical Engineering
Purdue University
Lafayette, Indiana

1 Commanding Officer
U.S. Army Medical Research Laboratory
Fort Knox, Kentucky

2 Keats A. Pullen, Jr.
Ballistic Research Laboratories
Aberdeen Proving Ground, Maryland

1 Commander
Air Force Cambridge Research Laboratories
Laurence G. Hanscom Field
Bedford, Massachusetts
Attn: CRXL

1 Director
U.S. Army Human Engineering Laboratories
Aberdeen Proving Ground, Maryland

5 Scientific & Technical Information Facility
P. O. Box 5700
Bethesda, Maryland
Attn: NASA Representative (S-AK/DL)

1 Mr. James Tippett
National Security Agency
Fort Meade, Maryland

1 Dr. Lloyd Hollingsworth
Director, ERD
AFCRL
L. G. Hanscom Field
Bedford, Massachusetts

1 Major William Harris
Electronics Systems Division
L. G. Hanscom Field
Bedford, Massachusetts

1 Instrumentation Laboratory
Massachusetts Institute of Technology
68 Albany Street
Cambridge 39, Massachusetts
Attn: Library W1-109

1 Research Laboratory of Electronics
Massachusetts Institute of Technology
Cambridge 39, Massachusetts
Attn: Document Room 26-327

1 Dr. Robert Kingston
Lincoln Laboratories
Lexington, Massachusetts

1 Lincoln Laboratory
Massachusetts Institute of Technology
P. O. Box 73
Lexington 73, Massachusetts
Attn: Library, A-082

1 Sylvania Electric Products Inc.
Electronic Systems
Waltham Labs. Library
100 First Avenue
Waltham 54, Massachusetts

1 Minneapolis-Honeywell Regulator Co.
Aeronautical Division
2600 Ridgeway Road
Minneapolis 13, Minnesota
Attn: Mr. D. F. Elwell
Main Station: 625

1 Inspector of Naval Material
Bureau of Ships Technical Representative
1902 West Minnehaha Avenue
St. Paul 4, Minnesota

20 Activity Supply Officer, USAELRDL
Building 2504, Charles Wood Area
Fort Monmouth, New Jersey
For: Accountable Property Officer
Marked: For Inst. for Exploratory Research
Inspect at Destination
Order No. 5776-PM-63-91

1 Commanding General
U.S. Army Electronic Command
Fort Monmouth, New Jersey
Attn: AMSEL-RE

1 Mr. A. A. Lundstrom
Bell Telephone Laboratories
Room 2E-127
Whippany Road
Whippany, New Jersey

1 AFMDC (MDSGP/Capt. Wright)
Holloman Air Force Base
New Mexico

1 Commanding General
White Sands Missile Range
New Mexico

1 Microwave Research Institute
Polytechnic Institute of Brooklyn
55 John Street
Brooklyn 1, New York

1 Cornell Aeronautical Laboratory, Inc.
4455 Genesee Street
Buffalo 21, New York
Attn: J. P. Desmond, Librarian

1 Sperry Gyroscope Company
Marine Division Library
155 Glen Cove Road
Carle Place, L.I., New York
Attn: Mrs. Barbara Judd

1 Rome Air Development Center
Griffiss Air Force Base
New York
Atten: Documents Library
RAALD

1 Library
Light Military Electronics Department
General Electric Company
Armament & Control Products Section
Johnson City, New York

1 Columbia Radiation Laboratory
Columbia University
538 West 120th Street
New York 57, New York

1 Mr. Alan Barnum
Rome Air Development Center
Griffiss Air Force Base
Rome, New York

1 Dr. E. Howard Holt
Director
Plasma Research Laboratory
Rensselaer Polytechnic Institute
Troy, New York

3 Commanding Officer
U.S. Army Research Office (Durham)
Box CM, Duke Station
Durham, North Carolina
Attn: CRD-AA-1P, Mr. Ulsh

1 Battelle-DEFENDER
Battelle Memorial Institute
505 King Avenue
Columbus 1, Ohio

1 Aeronautical Systems Division
Navigation and Guidance Laboratory
Wright-Patterson Air Force Base
Ohio

1 Aeronautical Systems Division
Directorate of Systems Dynamic Analysis
Wright-Patterson Air Force Base
Ohio

1 Commanding Officer (AD-5)
U.S. Naval Air Development Center
Johnsville, Pennsylvania
Attn: NADC Library

2 Commanding Officer
Frankford Arsenal
Philadelphia 37, Pennsylvania
Attn: SMUFA-1300

1 H. E. Cochran
Oak Ridge National Laboratory
P. O. Box X
Oak Ridge, Tennessee

1 U.S. Atomic Energy Commission
Office of Technical Information Extension
P. O. Box 62
Oak Ridge, Tennessee

1 President
U.S. Army Air Defense Board
Fort Bliss, Texas

1 U.S. Air Force Security Service
San Antonio, Texas
Attn: ODC-R

1 Director
Human Resources Research Office
The George Washington University
300 North Washington Street
Alexandria, Virginia

20 ASTIA Technical Library AFL 2824
Arlington Hall Station
Arlington 12, Virginia
Attn: TISLL

1 Commander
U.S. Army Research Office
Highland Building
3045 Columbia Pike
Arlington 4, Virginia

1 U.S. Naval Weapons Laboratory
Computation and Analysis Laboratory
Dahlgren, Virginia
Attn: Mr. Ralph A. Niemann

2 Army Material Command
Research Division
R & D Directorate
Bldg. T-7
Gravelley Point, Virginia